



A Model of a Temporal Filter in Chemoreception to Extract Directional Information from a Turbulent Odor Plume

Paul Moore; Jelle Atema

Biological Bulletin, Vol. 174, No. 3. (Jun., 1988), pp. 355-363.

Stable URL:

<http://links.jstor.org/sici?sici=0006-3185%28198806%29174%3A3%3C355%3AAMOATF%3E2.0.CO%3B2-N>

Biological Bulletin is currently published by Marine Biological Laboratory.

Your use of the JSTOR archive indicates your acceptance of JSTOR's Terms and Conditions of Use, available at <http://www.jstor.org/about/terms.html>. JSTOR's Terms and Conditions of Use provides, in part, that unless you have obtained prior permission, you may not download an entire issue of a journal or multiple copies of articles, and you may use content in the JSTOR archive only for your personal, non-commercial use.

Please contact the publisher regarding any further use of this work. Publisher contact information may be obtained at <http://www.jstor.org/journals/mbi.html>.

Each copy of any part of a JSTOR transmission must contain the same copyright notice that appears on the screen or printed page of such transmission.

JSTOR is an independent not-for-profit organization dedicated to creating and preserving a digital archive of scholarly journals. For more information regarding JSTOR, please contact support@jstor.org.

A Model of a Temporal Filter in Chemoreception to Extract Directional Information From a Turbulent Odor Plume

PAUL MOORE AND JELLE ATEMA

*Boston University Marine Program, Marine Biological Laboratory,
Woods Hole, Massachusetts 02543*

Abstract. We ask whether animals can derive spatial information from temporal patterns contained in turbulent odor plumes under realistic biological constraints of receptor properties (size and physiological responses) and behavioral requirements (time averaging). We modeled an appropriately scaled aquatic odor plume with a salt tracer to serve as the input to two different lobster chemoreceptor organs.

We then constructed a computer model based on some of the currently known temporal filtering characteristics of lobster chemoreceptor cells *in situ*. The output of this model represents the supra-threshold stimulus intensity fluctuations “seen” by realistically adapting cells. The input and output of the model were evaluated for directional information. We focused on four parameters that characterize concentration peaks within the plume: *height*, *length*, *maximum rising slope*, and *off time* (time between peaks). These characteristics were analyzed under two biologically important sampling strategies: one corresponding to a *continuous*-sampling receptor organ (*e.g.*, lobster leg, catfish nose) and the other to a *discrete*-sampling receptor organ (*e.g.*, lobster nose, tuna nose). We let the discrete-sampling model analyze at a frequency of four sniffs per second, each averaging over 100 ms. The continuous-sampling model used an historic exponential average of 25, 100, or 1000 ms based on disadaptation rates of receptor cells *in situ*.

In this preliminary study, filtered odor spectra contained less biologically useful information than the unfiltered input spectra. Discrete and continuous models were not different. In all cases, the probability distribu-

tion of maximum rising slopes of stimulus concentration contained the most reliable directional information.

Introduction

Various terrestrial and aquatic animals show remarkable abilities to orient in turbulent odor plumes. Considering the non-directionality of odor signals *per se*, we hypothesized that turbulent odor dispersal processes might create spatial patterns that could serve as directional cues, and that chemoreceptor organs may have temporal filter properties that match dominant spatial frequencies of odor plumes at size scales relevant to the animals and their receptor organs (Atema, 1985, 1988; Derby and Atema, 1988). Dispersal of an odor into a fluid volume occurs over a wide range of size scales. At size scales less than 1–10 mm, molecular diffusion determines the distribution of odor in the environment, whereas at scales larger than 1–10 mm advection dominates the dispersal process. Aquatic systems are likely to be turbulent at scales larger than 10 mm. This is the size scale of most macroscopic animals.

While turbulence is chaotic and thus not predictable at any instant in time or space, it has predictable patterns when spatial and/or temporal averages are taken. Mean distributions of turbulent odor dispersal can be predicted by Sutton's model (1953). This model is based on a continuously and constantly emitting odor source and assumes that the average odor concentration will follow a normal (Gaussian) distribution in any plane perpendicular to the down-current axis. The time-averaged odor plume increases in area and decreases in concentration exponentially with distance from the source. This model describes a continuous (non-patchy) odor distribution

within the plume. To establish a reasonable approximation to a Gaussian distribution under the conditions considered by Sutton, an averaging time of several minutes is required (Pasquill, 1961; Gifford, 1968; Miksad and Kittredge, 1979; and Elkinton, *et al.*, 1984). Predicting animal responses from such time-averaged models has proven inadequate in some cases; when orientating toward the source of a pheromone plume, gypsy moths did not appear to time-average on the same scale as the Sutton model (David *et al.*, 1982; Elkinton *et al.*, 1984). It is obvious that animals do not always have the "luxury" of waiting a few minutes to take an average! They may have to make behavioral decisions in as short a time period as the circumstances demand. This requires analysis of more instantaneous parameters of odor plumes.

The instantaneous distribution of odor within a turbulent odor plume is quite different from Sutton's (1953) time-averaged distribution (Wright, 1958; Aylor, 1976; Aylor *et al.*, 1976; Shorey, 1976; and Murlis and Jones, 1981). Instantaneous plumes meander, and break up into filaments and patches. Instantaneous odor distributions follow local environmental turbulence. Turbulent eddies occur simultaneously over a range of sizes. The largest eddies pass down their energy into smaller and smaller eddies until the energy finally dissipates. Eddies of the size scale of an odor filament cause it to break up into patches; smaller eddies redistribute the odor within the patches and cause decreases in the odor concentration gradients at patch edges; larger eddies move the entire odor plume and cause meandering. For a more complete description of Gaussian and instantaneous odor plumes see Elkinton and Cardé (1984). The result of a patchy odor distribution is that an animal located downwind of an odor source will experience periods of odor concentration well above and below the mean concentration.

Measurements of the instantaneous structure of odor plumes are needed to understand which dynamic characteristics of the plume are the best indicators for orientation within the plume. These measurements must be made at spatial and temporal sampling scales an order of magnitude greater than those relevant to chemoreceptors or the animal behavior under consideration: different animals and different receptor organs have their own characteristic time and space scales (Atema, 1985, 1988). At present, spatial scales for receptor organs must be estimated from their morphology and in some cases from preliminary data on flow fields (Vogel, 1983; Moore and Atema, unpub.). Temporal scales relevant to chemoreceptor organs are poorly known; they must be estimated from still-rare physiological response data (Kaissling *et al.*, 1987; Voigt and Atema, 1987a, b; Christensen and Hildebrand, 1988). Eventually, models must be adjusted to accommodate these species-specific scales.

Our study was designed to measure odor dispersal at the sampling scales of two lobster (*Homarus americanus*) chemoreceptor organs, the antennules (olfaction) and legs (taste). To model an odor plume at a size scale of relevance to a lobster we chose a velocity and volume similar to the filter feeding current of a single mussel *Mytilus edulis*, a common prey of lobsters. A filter-feeding mussel generates a turbulent odor plume of metabolites; this plume is carried away and redistributed by ocean currents. The pumping rates of *M. edulis* range from 0 to 50 ml/min (Kirby-Smith, 1972; Winter, 1978). The model plume was generated by continuous injection of a salt tracer ("the mussel") in a fresh water flume ("the ocean").

For *H. americanus*, odor cues appear to be more important than rheotaxis in orientation to distant odor sources (McLeese, 1973). Since removal of one lateral antennule results in random direction choice, directional decisions seem to be based on a comparison of input from the two lateral antennules (Devine and Atema, 1982). Similar results were obtained in odor orientation experiments with the spiny lobster, *Panulirus argus* (Reeder and Ache, 1980).

Flicking of the lateral antennules decreases the boundary layer around the dense clusters of 1 mm long aesthetasc sensilla (Snow, 1973; Moore and Atema, unpub. obs.) and appears to be the functional equivalent of vertebrate sniffing. Flicking probably determines the spatial and temporal frequency filtering of the chemoreceptor cells of the antennule (Schmitt and Ache, 1979; Atema, 1985). *H. americanus* antennules can flick with burst rates of 4 s^{-1} (pers. obs.). Once in the general vicinity, lobsters use their legs to locate and recognize food; for this, leg chemoreception is essential (Derby and Atema, 1982). Legs wave but do not flick: they seem to sample odor plumes continuously.

The exact sampling frequency and volume relevant to lobster chemoreceptors are not yet known. Temporal filters result from boundary layer plus cellular adaptation (Borroni and Atema, 1987) and disadaptation rates (Voigt and Atema, 1987a, b). From these data and response rates obtained in insect pheromone receptor cells (Kaissling *et al.*, 1987; Christensen and Hildebrand, 1988), we estimate that lobster leg receptors might follow pulse rates of $0.1\text{--}10 \text{ s}^{-1}$. Spatial scales are estimated to be on the order of 1–10 mm. To resolve slopes of concentration peaks, *i.e.*, rate of increase of odor concentration, we sampled the odor plume at 40 s^{-1} , an order of magnitude faster than the estimated sampling (*i.e.*, flicking) frequency of our biological filters under study.

We analyzed our "model plume" with the two different sampling methods: *continuous i.e.*, the slow movements of a lobster leg, and *discrete i.e.*, the fast flicking of lobster antennules. These two sampling methods also

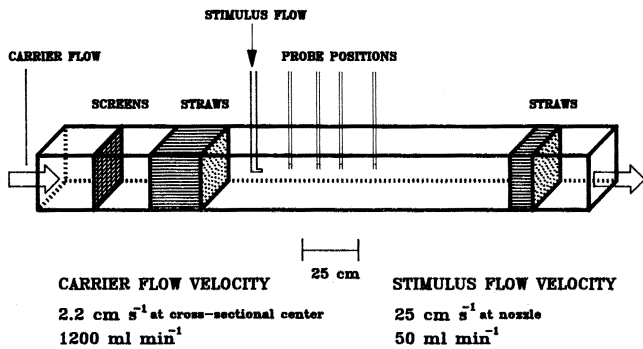


Figure 1. Diagram of flume used for salt plume turbulence measurements at the size and time scale of lobster chemoreceptor organs. Probes shown at each of the four sites; only one probe was in the water during the measurements, all taken in the cross-sectional center of the plume.

exist in the functional designs of fish noses. Fish have been classified (Døving *et al.*, 1977) as isosmates (continuous ciliary flow, *e.g.*, catfish) and cyclosmates (“sniffing” via accessory pumps and muscles, *e.g.*, tuna). Overall, our model was designed to represent the stimulus pulse patterns that a chemoreceptor cell *in situ* with known temporal filter characteristics might detect within the odor plume emanating from a pumping mussel located a short distance upcurrent. The first generation model is meant to define critical parameters, particularly those for which little or no information is yet available.

Materials and Methods

Plume model

To generate the model plume we used a 248 cm × 34 cm × 23 cm flume with a tap water flow ($1.2 \pm .21/\text{min}$) (Fig. 1). This carrier flow passed through three sheets of window screen, and a collimator of 5 mm diameter soda straws 22 cm long. The test area was 142 cm long. Another row of 10-cm long soda straws was placed before the outflow tube. The flow velocity in the center of the test area was 2.2 ± 0.2 cm/s measured by timing the movement of a patch of dye.

The tracer plume was a 0.7% NaCl solution injected at 50 ± 1 ml/min. into the test area of flow through a Pasteur pipette with 1 mm ID tip opening. Flow velocity at the nozzle was 25 cm/s ($Re \approx 500$). The nozzle of the pipette was 10 cm down-stream from the collimator, 7 cm from the bottom and equidistant from the sides. A dye was mixed in with the salt solution to visually locate the plume center line. Although the tracer was somewhat denser than the surrounding water, it did not drop significantly over the sampling area.

As an indicator of instantaneous salt concentration we measured conductivity (YSI model #35) around two sil-

ver wire (gauge 30) electrodes each with an exposed length of 1 cm. The wires were spaced 1 cm apart to give a spatial sampling area of 1 cm². These dimensions were chosen to approximate the 1 ml estimated sample volume of one lobster flick, or the slow flow volume immediately surrounding a lobster leg. The output from the conductivity meter was monitored on a chart recorder (Gould Brush model #220) and recorded on an FM tape recorder (Vetter model D) for later computer analysis.

Salt concentrations were measured at four sites, each in the center line of the plume: 12.5, 25, 34.5, and 50 cm from the pipette mouth. The plume center line was located by first sighting the dye. Once the probe was positioned it was left there for 1.5 min before recording a 7.5 min sample. One 7.5 min sample was taken at each site.

The four 7.5-min analog samples were replayed from the tape recorder through an AD converter into a IBM PC computer. The sampling rate of the computer was set at 40 s⁻¹, *i.e.*, the computer sampled the tape every 25 ms for 9 ns to derive a data point. Although the 40 s⁻¹ rate was chosen to be 10× the lobster flicking sample rate it also represented, perhaps fortuitously, the maximum frequency of turbulence in the plume without including high frequency noise of the recording system.

A set of known and fixed salt concentrations were recorded and played through the AD converter to construct a calibration curve for the entire salt concentration recording system. This allowed the computer voltage data to be expressed as actual salt “stimulus” concentrations.

The salt plume appeared as a series of concentration peaks of varying strength and duration. They represent a typical turbulence spectrum (Murlis and Jones, 1981; Atema, 1985). As expected the peaks flattened with distance downstream from the source (Fig. 2). These turbulence spectra were used as the input data for our receptor filter model.

Receptor filter model

For the discrete-sampling “nose” we assumed that the receptors will average the sample over a period of 100 ms (approximate time for the down-stroke of the antennule) and then “wait” 150 ms while the antennule recovers for the next downstroke. Preliminary observations (unpub.) showed that the down-stroke thoroughly mixes the odor distribution in the sampling space. Therefore, we used a centered arithmetic mean of the concentrations encountered over the 100 ms sample period. For the continuous sampling nose, we assumed it averages over 25 ms.

Receptor cells adapt and disadapt as they sample. For initial simplicity, we base this model on data from self-adaptation experiments, *i.e.*, adaptation to the same compound(s). The instantaneous adaptation state of a

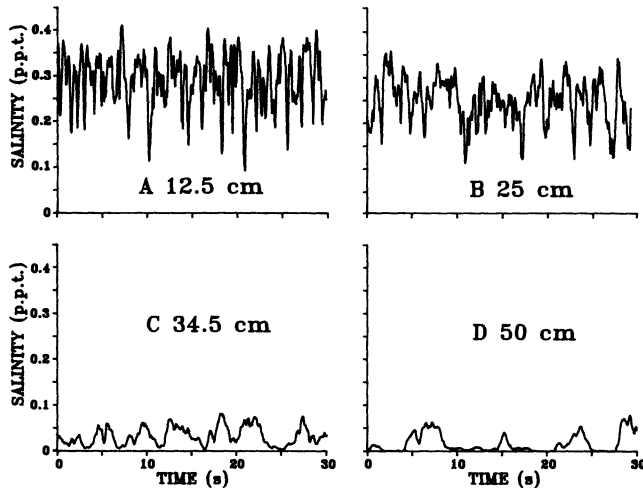


Figure 2. Typical turbulence spectra of salt concentrations in the plume. Random 30 s segments from 7.5 minute recordings, one at each site. A–D: Distances from the pipette mouth to the plane of the electrodes. The plume changes its turbulent character rather abruptly between 25 and 34.5 cm. It is not until 50 cm from the source that the larger scale turbulence causes sufficient meander to result in periods of zero signal.

receptor cell is measured as its response threshold and is dependent on past concentrations sampled. We assumed that receptor cells self-adapt within seconds (see Borroni and Atema, 1987, and in prep.) and for this model we use instantaneous and complete adaptation immediately following any sample period (*i.e.*, 100 ms for discrete sampling and 25 ms for continuous sampling). Previously encountered concentrations will have cumulative effects on the current adaptation state of the cell. We considered a total period of effectiveness of $T = 10$ s, an estimate based on the disadaptation time course of taurine and glutamate receptor cells *in situ* which range from 2.5–40 s for complete disadaptation from a 1-s glutamate or taurine pulse 1–3 log steps above a taurine or glutamate background (Voigt and Atema, 1987a, b). The magnitude of these effects depends on the magnitude of the previously sampled concentrations and the time (t in s) since their occurrence. We assumed that the effect of a previous concentration upon the cell's instantaneous adaptation state decays exponentially with time. Based on the presumed disadaptation time course of taurine and glutamate receptor cells *in situ*, we generated equation 1 to determine the weight factor (W_t) by which the response of the cell at $t = 0$ should be reduced due to each of the 40 samples in the previous period ($T = 10$ s).

$$W_t = \exp(1 + 0.4 \times (T - t))/100 \quad (1)$$

The numbers 1, .4, and 100 were chosen to scale the height and rate of decay of the curve to the height and time scale of the input data. This model assumes that

all previous samples contribute to the current adaptation state of the receptor cell—even those that did not result in output from the cell (*e.g.*, Fig. 3, subthreshold sample bar at $t = -2$, etc.). In addition, for the sake of simplicity, we used the unmodified input data as the basis for each new point. (In doing so we did not take into account possible interactive effects that may exist between samples, *e.g.*, strong pulses early in the period T reduce the stimulating effectiveness of pulses later in the period T due to biochemical adaptation of the cell; if adaptation is a result of excitation, these strong pulses may then reduce the effectiveness of later pulses in suppressing the response at $t = 0$).

W_t was used as the weight factor in a “historical” weighted mean (A) in equation 2:

$$A = \Sigma(C_t \times W_t) / \Sigma W_t \quad (2)$$

where A is the adaptation state of the receptor at time t , and C_t is the stimulus concentration at time t . The weight portion ($W_t / \Sigma W_t$) of equation 2 is visualized in Figure 3 (dotted curve). This curve reflects the amount of adaptation (= threshold increase) that the 40 sample bins prior

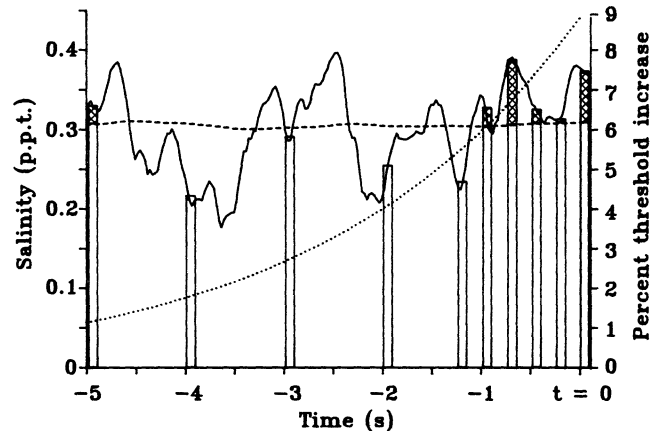


Figure 3. Five second sample of salt plume concentration spectrum (solid curve; salinity in ppt) and sampling bins (vertical bars) from discrete sampling model. Total height of a bar represents mean unfiltered concentration encountered during sample period; width of bar represents sampling time bin (one flick = 100 ms). Cross-hatched portion of bar represents perceived concentration, *i.e.*, above the cell's instantaneous threshold (= adaptation level: broken line) caused by previous samples taken. The model assumes constant flicking at 4 s^{-1} ; for clarity not all sample bins are shown, except in the last 1.5 s. Only sampled concentrations contribute to adaptation; concentrations in between sample periods go “unnoticed.” In this example, a hypothetical cell with 10 s disadaptation time is used; the exponential function (dotted line) represents the time-dependent amount of suppression (% of response at $t = 0$) caused by preceding stimuli: recent samples (*e.g.*, $t = -1$) have greater effects (6.2% of sample at $t = -1$) on the response at $t = 0$ than earlier samples (*e.g.*, $t = -5$; 1.1% of sample value at $t = -5$); samples prior to $t = -10$ no longer affect the response to a sample at $t = 0$.

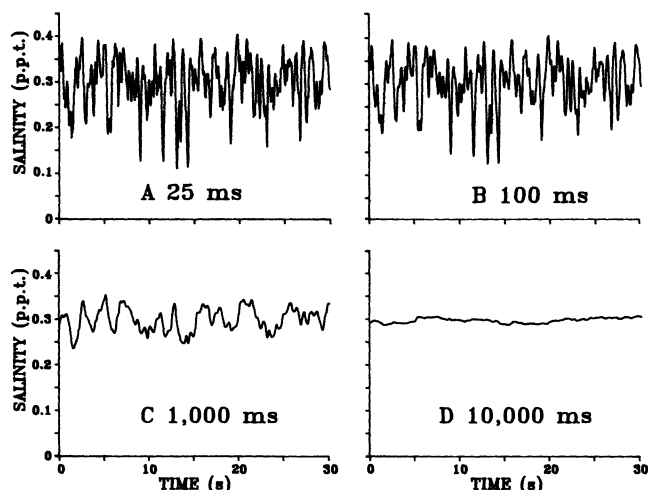


Figure 4. Concentration spectra from the 12.5 cm sample site (Fig. 2A) filtered with different disadaptation times. A. Unfiltered spectra (from Fig. 2A). B, C, D. Spectra representing instantaneous adaptation state of these different receptor cells with very fast (B), fast (C), and slow (D) disadaptation characteristics. Disadaptation time is based on the assumptions of instantaneous adaptation and an exponential disadaptation time course as shown in Figure 3. The 10,000 ms filter results in a smooth concentration average similar to the broken line of Figure 3.

to $t = 0$ contribute to the overall adaptation state at $t = 0$. In Figure 3 we visualize a series of “flicks” as they sample the input concentration profile (solid line). The response to a pulse at $t = 0$ is affected by the cell’s exposure to a series of previous concentrations (measured in 100 ms sample bins every 250 ms for 10 s). The effect of each of the previously sampled concentrations is given by an exponentially decaying function from $t = 0$ to $t = -10$ s. For example, the sample bar at $t = -5$ registered 0.33 ppt salinity; it raises the threshold at the $t = 0$ sample by about 1% or 0.0033 ppt. The sample at $t = -1$ registered about the same salinity but, being more recent, its effect on raising the threshold at $t = 0$ is 6% or 0.0198 ppt. The sum effect of all samples during T causes the cell’s threshold to be raised: the hatched portion of the bar is supra-threshold. The threshold curve (broken line of Fig. 3) represents a moving average of points generated as described above.

For the continuous sampling filter model we assumed that the receptor cell integrates over a fixed (*e.g.*, 25 ms) time bin, then integrates over the immediately following 25 ms bin, etc. The samples taken in previous time bins influence the response to the sample at $t = 0$ as in the discrete sampling model except that now the bins follow each other directly. We chose disadaptation times of $T = .1, 1, \text{ and } 10$ s for the continuous sampling model. Thus, with the input data sampled every 25 ms, the .1 s (100 ms) disadaptation time bin contains four points, 1

s contains 40 points, and the 10 s contains 400 points (Fig. 4).

To analyze peak characteristics of the odor plume we had to define a peak and assign a baseline, *i.e.*, a stimulus background level to which a real receptor cell would be adapted. The background is evident when stimulus concentrations return to undetectable levels after a burst of stimulus pulses (Fig. 2D). However, when pulses continue to follow so rapidly that stimulus concentrations remain elevated between pulses (Fig. 2A, B) we must adopt a quantitative rule for a background. We chose the background levels that result from integration over 10 s, *i.e.*, the cell was assumed to see peaks superimposed on one of the concentration averages of Figure 5. A peak is then defined as starting and ending at the appropriate background. In addition, only when the concentration value between two peaks dropped below 30% of the height of the previous peak, were the peaks considered separate.

For both the discrete and continuous model, four stimulus peak parameters were measured: *height*, from the maximum value of the peak to background; *length*, from beginning to ending of peak as defined above; *off time*, time from the end of one peak to the beginning of the next peak; and *maximum slope* on the rising side of the peak, calculated as the maximum value of the double linear concentration-time tangent, measured as ppt per 25 ms sample bin. Examples of these are shown in Figure 6.

Results

Since the number of samples taken for making a directional decision by animals orienting in a plume might

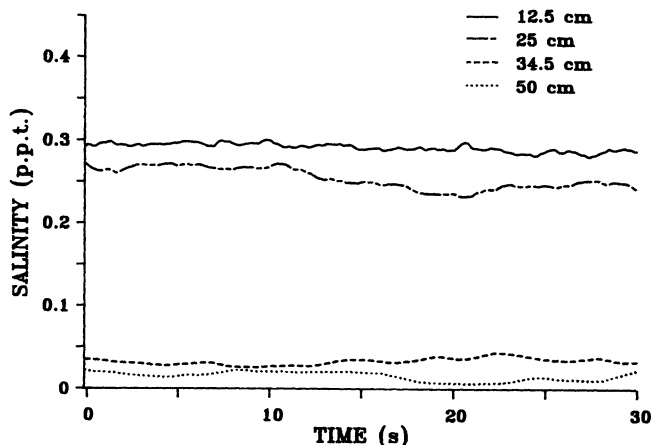


Figure 5. Concentration spectra at each of the four sample sites (Fig. 2) at an averaging time of 10,000 ms (10 s). This low-pass filter results in a “mean stimulus concentration.” These means represent the cell’s response threshold in the stimulus conditions of the four sites; they were used as baselines for peak measurements.

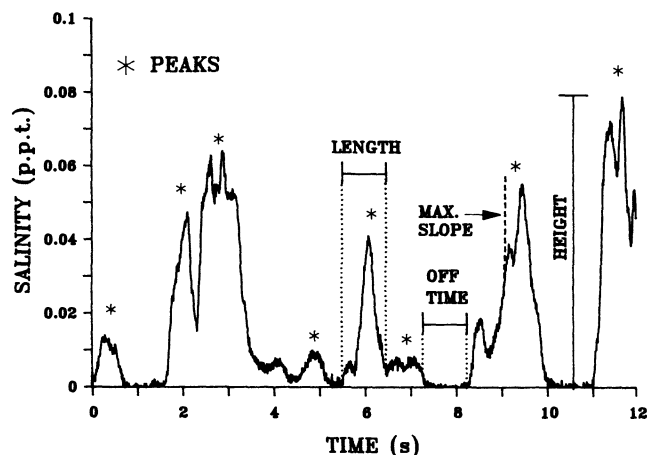


Figure 6. Unfiltered salt plume spectra from 50 cm site demonstrating the peak parameters analyzed. *Peak height*, measured against a baseline (Fig. 5) reflecting the presumed adaptation state of the receptor (baseline shown here: zero). *Peak length*, time from the beginning to ending of peak (see text). *Off time*, time of no signal, between successive peaks. *Peak slope*, maximum slope on the rising side of the peak.

be small (for chemoreception in the order of seconds) compared with our 7.5 min sample, we plotted probability distributions of the four peak parameters. The distributions were calculated over the entire 7.5 min sample. Probability distributions reveal those characteristics of an odor plume that change most reliably with distance, and hence might provide directional information. The probability distributions of peak parameters from the discrete sampling model (Fig. 7) show that the most reliable source of directional information is contained in the maximum slope distribution (Fig. 7A). Approximately 85% of the slope values encountered at the closest two sites are not encountered at the farthest two sites. The closest two sites have more sharply rising slopes, while the other two sites have shallower slopes. The two near sites have nearly indistinguishable characteristics as do the two far sites. We know nothing about the slope discrimination ability of the actual chemoreceptor system.

The peak height distribution (Fig. 7B) provides less directional information than peak slope distribution. Peak height values at the farthest two sites range from 0–0.06 ppt. This same range of heights occurs 65% of the time at the closest two sites. This means that directional information is present in only 35% of the peak heights encountered; and this does not take into account the inaccuracy of height discrimination present in the receptor system. This overlap in the probability distributions is also present in the off times, 70%, (Fig. 7C) and peak lengths, 60%, (Fig. 7D).

Similar results were obtained in the continuous flow model (Fig. 8). The greatest separation in distributions among the four parameters occurs with the peak slopes

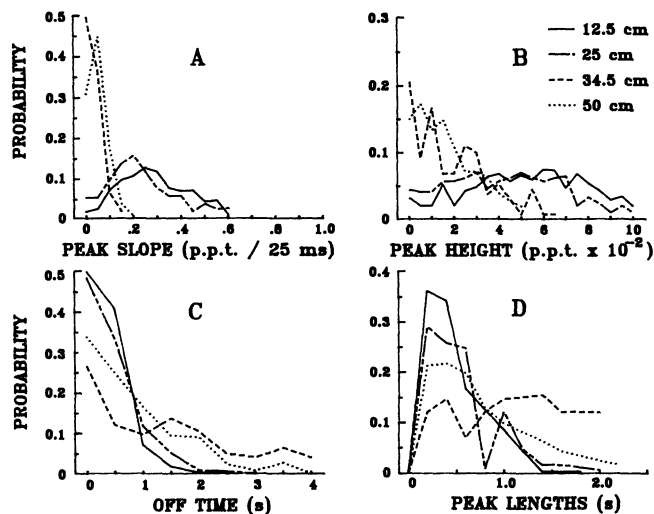


Figure 7. Probability distributions of peak parameters from the discrete sampling model with a very fast disadaptation time of 100 ms. A. Peak slope B. Peak height C. Off time D. Peak length.

(Fig. 8A). The overlap among the four sites is approximately 15%. The overlap in the distributions of the other three parameters is 73% (peak heights), 70% (off time), and 48% (peak lengths) (Figs. 8B, C, and D, respectively).

The probability distributions of peak slopes for different disadaptation times (25, 100, 1000 ms) reflect, as expected, that concentration peaks become smoother as the disadaptation time of the receptor cell *in situ* increases (Figs. 9A, B, C). However, this overall change in slope does not change the relative amount of overlap of the four distributions; this stays surprising constant around 15%. Since this overlap stays constant with

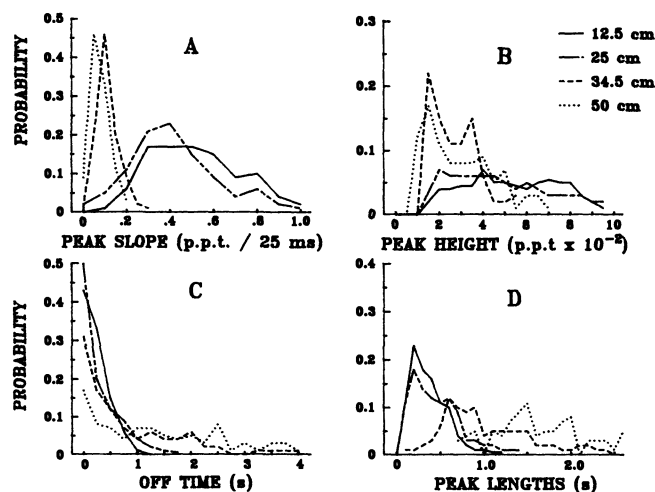


Figure 8. Probability distributions of the four peak parameters from the continuous sampling model with a disadaptation time of 100 ms (Fig. 5B). A. Peak slope B. Peak height C. Off time D. Peak length.

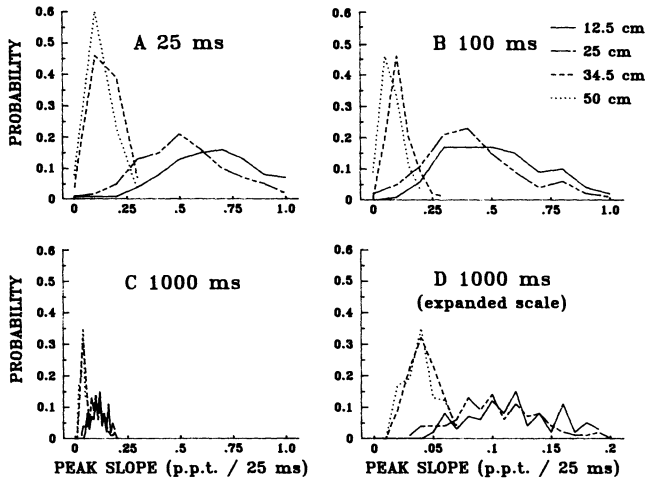


Figure 9. Effect of averaging time on the probability distribution of maximum peak slopes representing chemoreceptors with different disadaptation times (A, B, C) from the continuous flow model. D is an expanded version of C.

changing disadaptation times, the potential directional information content of the parameter stays constant also. The same was found for the other three peak parameters. Therefore, receptor cells with different averaging periods cannot improve on this situation.

Discussion

This study accomplished two goals. First, we measured the turbulent spectrum in an odor plume scaled such that it might be realistic for a lobster searching for an odor source. Both the spatio-temporal scale of the plume itself and the spatial average taken by the "receptor," *i.e.*, the electrode size and spacing, were lobster-like. Second, we constructed a first-generation temporal filter model that reflects the biological reality that receptor cells adapt to ambient concentrations where electronics do not unless specifically instructed. Our instructions were based on preliminary physiological data on self-adaptation and disadaptation rates of chemoreceptor cells *in situ*, *i.e.*, including the boundary layer normally present. The filter model must be adjusted as physiological data and boundary layer measurements accumulate.

The turbulent spectrum of any plume is highly dependent upon the physical conditions of the environment. To develop this first model, we chose one specific plume condition: a constantly pumping mussel under one laminar carrier flow condition and we sampled only at four locations. In the future, extensive sampling must be done under various flow conditions and with different odor sources encountered in the natural environment of the *H. americanus*.

As the plume ages the physics of turbulent dispersal

changes the values of plume parameters, *i.e.*, peak slopes get less steep, peak heights fall, *etc.* From a spatial comparison of these changes, animals could estimate source distance and direction. Distance information might be used to assess if it is energetically worthwhile (considering hunger, predators, *etc.*) to proceed to the source or to stay put: the longer a plume has been in the environment the higher the probability that the source is gone, *e.g.*, a competitor may have found and exploited the source. In addition, animals that have no earth reference (such as visual or contact cues of the ground) to determine current direction may use spatial sampling of turbulent plumes to determine source direction. Our filter model can be used to analyze which properties of turbulent plumes and which physiological and behavioral sampling strategies provide the best information.

The strength of any model lies in its ability to rigidly define one's assumptions and hence show which assumptions do not correspond with biological or physical reality. One of these inconsistencies may already be apparent. We suggested (Atema, 1985, 1987, 1988) that temporal filter properties of chemoreceptor cells may be matched to those dominant spatial frequencies of turbulence that contain important biological information. We had thus expected that filtered turbulence spectra would contain more directional information. Instead we found less separation in the filtered probability distributions of peak slopes than in the unfiltered distribution (Fig. 10). Since the biological assumption of matching of filters seems reasonable and is found in many other sensory systems we must first examine and refine the model before concluding that chemoreceptors are exceptionally constrained by the physics of the microenvironment (De Simone, 1981) or perhaps by the biochemical processes of sensory transduction.

Various assumptions must be re-evaluated in light of

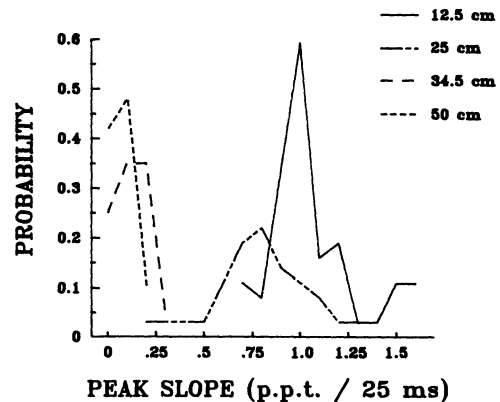


Figure 10. Probability distribution of unfiltered peak slopes (Fig. 2) continuously sampled every 25 ms at the four sample sites, against an absolute 0.02 ppt salinity threshold.

future physiological results. There is insufficient knowledge of the adaptation and disadaptation time courses of various chemoreceptors and, in particular, on the contribution of the boundary layer. This affects the adaptation level of the cells against which peaks are measured. "Peak height against background" may be a more important parameter for orientation than we conclude from the current model. Furthermore, if cell excitation determines its level of adaptation then we must revise the exponential function (1) we used here, and use response output, not stimulus input, as the basis from which to calculate adaptation state. Finally, we know nothing about the time over which chemoreceptor cells integrate. Some photoreceptors integrate over 500 ms under very low photon density conditions (Fein and Szuts, 1982). Our 25–1000 ms assumption for chemoreceptors may or may not be realistic. It corresponds to fast reaction times measured elsewhere (Kelling and Halpern, 1983). If boundary layers form the rate limiting factor determining response latency then data from very different chemoreceptor organs can be compared.

Chemoreceptor cells may function under rather severe physical constraints. Every interface between a solid and a fluid, be it air or water, results in a boundary layer (Tritton, 1977; Vogel, 1981). Close to the solid surface fluid motion approaches zero velocity. Chemical stimuli can penetrate through this inner portion of the boundary layer only by molecular diffusion. The thickness of this diffusion layer may be a critical constraint not only on response latency (De Simone, 1981) but also on the temporal resolution of chemoreceptor cells since diffusion time increases geometrically with distance. Latency and temporal resolution are obviously related. A diffusion layer will act as an integrating filter, and hence a low pass filter, reducing the frequency response of the receptor system to lower frequencies than those present in the free flow around the organ (Fig. 2). The critical difference between flicking and non-flicking may be reduction of the boundary layer by high-velocity flicks. The present analysis showed no significant difference in discrete and continuous sampling. This may change with more extensive analysis of different plumes and more refined assumptions. Measurements of boundary layers under biologically realistic conditions must be made, and the results added to this model as integrating filters with diffusion layer thickness as a parameter. To this must be added the subsequent diffusion distances from the surface of the receptor organ to the receptor site requiring accurate morphological measurements of receptor sensilla. The remaining filtering is then probably due to biochemical processes.

This model and its subsequent refinements can be used to describe and analyze different odor plumes extensively. This will give insight into those turbulent fea-

tures that are most suitable for biological use given the intrinsic constraints of chemoreceptor physiology and morphology. Animal behavior may become involved as an animal searches an odor plume for useful features. In this context it may be interesting to refer to the sudden difference in turbulent spectra between the two very similar near sites and the two quite similar far sites (Figs. 2, 5, 7, 8, 9, 10). Such sudden breaks are not uncommon in turbulent plumes and may serve as useful biological indicators of nearness to the source. In general, we expect that this model will help us see to what degree the physics of the environment constrain the ability of chemoreceptors to extract spatial and temporal features of natural odor distributions that might be useful for orientation.

Acknowledgments

We thank Dr. Rainer Voigt for his valuable assistance throughout the study. Supported by grants from the Whitehall Foundation and NSF (BNS 8512585) to JA and a Presidential University Graduate Fellowship from Boston University to PM. Earlier spectrographic measurements of aquatic odor plumes were made by Atema, Murray-Brown, and Bryant (1982 unpub.), described in Atema (1985).

Literature Cited

- Atema, J. 1988. Distribution of chemical stimuli. Pp. 29–56 in *Sensory Biology of Aquatic Animals*. J. Atema, A. N. Popper, R. R. Fay, and W. N. Tavolga, eds. Springer-Verlag, NY.
- Atema, J. 1987. Chemoreceptor adaptation: a patch in space is a pulse in time. *Chem. Senses* 12: 189–190.
- Atema, J. 1985. Chemoreception in the sea: adaptation of chemoreceptors and behavior to aquatic stimulus conditions. *Soc. Exp. Biol. Symp.* 39: 387–423.
- Aylor, D. E. 1976. Estimating peak concentrations of pheromones in the forest. Pp. 177–188 in *Perspectives in Forest Entomology*, J. E. Anderson, and M. K. Kaya, eds. Academic Press, NY.
- Aylor, D., J.-Y. Parlange, and J. Granett. 1976. Turbulent dispersion of disparlure in the forest and male gypsy moth response. *Environ. Entomol.* 10: 211–218.
- Borroni, P. F., and J. Atema. 1987. Self- and Cross-adaptation of single chemoreceptor cells in the taste organs of the lobster, *Homarus americanus*. In *Olfaction and Taste IX*, S. Roper and J. Atema, eds. N.Y. Acad. Sci. 510: 184–186.
- Christensen, T. A., and J. G. Hildebrand. 1988. Frequency coding by central olfactory neurons in the sphinx moth *Manduca sexta*. *Chem. Senses* 13: 123–130.
- David, C. T., J. S. Kennedy, A. R. Ludlow, J. N. Perry, and C. Wall. 1982. A reappraisal of insect flight towards a distant, point source of wind-borne odor. *J. Chem. Ecol.* 8: 1207–1215.
- Derby, C. D., and J. Atema. 1988. Chemoreceptor cells in aquatic invertebrates: peripheral mechanisms of chemical signal processing in decapod crustacea. Pp. 365–385 in *Sensory Biology of Aquatic Animals*, J. Atema, A. N. Popper, R. R. Fay, and W. N. Tavolga, eds. Springer-Verlag, NY.
- Derby, C. D., and J. Atema. 1982. The function of chemo- and mechanoreceptors in lobster (*Homarus americanus*) feeding behavior. *J. Exp. Biol.* 98: 317–327.

- De Simone, J. A. 1981.** Physiochemical principles in taste and olfaction. Pp. 213–229 in *Biochemistry of Taste and Olfaction*, R. H. Cagan, and M. R. Kane, eds., Acad. Press, NY.
- Devine, D. V., and J. Atema. 1982.** Function of chemoreceptor organs in spatial orientation of the lobster, *Homarus americanus*: differences and overlap. *Biol. Bull.* **163**: 144–153.
- Dóving, K. B., M. Dubois-Dauphin, A. Holley, and F. Jourdan. 1977.** Functional anatomy of the olfactory organ of fish and the ciliary mechanism of water transport. *Acta. Zool.* **58**: 245–255.
- Elkinton, J. S., and R. T. Cardé. 1984.** Odor Dispersion. Pp. 73–91 in *Chemical Ecology of Insects*, W. J. Bell, and R. T. Cardé, eds. Sinauer Associates, Inc. Sunderland, MA.
- Elkinton, J. S., R. T. Cardé, and C. J. Mason. 1984.** Evaluation of time-average dispersion models for estimating pheromone concentration in a deciduous forest. *J. Chem. Ecol.* **10**: 1081–1108.
- Fein A., and E. Z. Szuts. 1982.** *Photoreceptors: Their Role in Vision*. Cambridge University Press, NY.
- Gifford, F. A., Jr. 1968.** An outline of theories of diffusion of lower layers of the plume dispersion model. *Int. J. Air Poll.* **3**: 253–260.
- Kaissling, K. E., C. Zack-Straussfeld, and E. Rumbo. 1987.** Adaptation processes in insect olfactory receptors: mechanisms and behavioral significance. In *Olfaction and Taste IX*, S. Roper and J. Atema, eds. N.Y. Acad. Sci. **510**: 104–112.
- Kelling, S. T., and B. P. Halpern. 1983.** Taste flashes: reaction times, intensity, and quality. *Science* **219**: 412–414.
- Kirby-Smith, W. W. 1972.** Growth of the bay scallop: the influence of experimental water currents. *J. Exp. Mar. Biol. Ecol.* **8**: 7–18.
- McLeese, D. W. 1973.** Orientation of Lobsters (*Homarus Americanus*) to odor. *J. Fish. Res. Board Can.* **30**: 838–840.
- Miksad, R. W., and J. Kittredge. 1979.** Pheromone aerial dispersion: a filament model. *14th Conf. Agric. and For. Met., Am. Met. Soc.* **1**: 238–243.
- Murlis, J., and C. D. Jones. 1981.** Fine-scale structure of odour plumes in relation to insect orientation to distant pheromone and other attractant sources. *Physiol. Entomol.* **6**: 71–86.
- Pasquill, F. 1961.** The estimation of the dispersion of wind-borne material. *Met. Mag.* **90**: 33–49.
- Reeder, P. B., and B. W. Ache. 1980.** Chemotaxis in the Florida spiny lobster, *Panulirus argus*. *Anim. Behav.* **28**: 831–839.
- Schmitt, B. C., and B. W. Ache. 1979.** Olfaction: response enhancement by flicking in a decapod crustacean. *Science* **205**: 204–206.
- Shorey, H. H. 1976.** *Animal Communication by Pheromones*. Academic Press, NY. 167 pp.
- Snow, P. J. 1973.** The antennular activities of the hermit crab, *Pagurus Alaskiensis* (Benedict). *J. Exp. Biol.* **58**: 745–766.
- Sutton, O. G. 1953.** *Micrometeorology*. McGraw-Hill, NY.
- Tritton, D. J. 1977.** *Physical Fluid Dynamics*. Van Nostrand Reinhold (UK) Co, Ltd., Wokingham, England. 362 pp.
- Vogel, S. 1983.** How much air passes through a silk moths antennae. *J. Insect Physiol.* **29**: 597–602.
- Vogel, S. 1981.** *Life in Moving Fluids: the Physical Biology of Flow*. Princeton University Press, Princeton, NJ. 352 pp.
- Voigt, R., and J. Atema. 1987a.** Spatial-temporal filtering in olfactory chemoreceptor cells. *Neurosci. Abstracts* **13**: 1407.
- Voigt, R., and J. Atema. 1987b.** Signal-to-noise ratios and cumulative self-adaptation of chemoreceptor cells. In *Olfaction and Taste IX*, S. Roper and J. Atema, eds., NY Acad. Sci. **510**: 692–694.
- Winter, J. E. 1978.** A review of the knowledge of suspension feeding in lamellibranchiate bivalves, with special reference to artificial aquaculture systems. *Aquaculture.* **13**: 1–33.
- Wright, R. H. 1958.** The olfactory guidance of flying insects. *Can. Entomol.* **80**: 81–89.